ARCHIVES
of
FOUNDRY ENGINEERING

ISSN (2299-2944)

10.24425/afe.2026.158014

Published quarterly as the organ of the Foundry Commission of the Polish Academy of Sciences

Selective Microwave Sintering of EPS Patterns for Lost Foam Casting

M. Topola [a], K. Jastrzębski [b], C. Rapiejko [a], P. Just [a]

[a] Department of Material Technologies and Production Systems, Faculty of Mechanical Engineering, Lodz University of Technology, Stefanowskiego Street 1/15, 90-924 Lodz-Poland

[b] Institute of Materials Science and Engineering, Faculty of Mechanical Engineering, Lodz University of Technology Stefanowskiego Street 1/15, 90-537 Lodz-Poland

* Corresponding author: E-mail address: mikolaj.topola@dokt.p.lodz.pl

Received 27.04.26; accepted in revised form 19.06.26; available online 31.08.2026

Abstract

This study investigates an innovative approach to sintering polystyrene via microwave radiation, aiming to transform manufacturing techniques in the lost-foam casting industry. The primary objective was to develop a laboratory-scale method for the microwave-based sintering of polystyrene patterns. Two types of polystyrene were examined: EPS Styropor P 426 Ccycled and EPS K-950w/S4311. The sintering process involved pre-expansion of the material with hot air, followed by placement in a 3D-printed mould, application of a water film as the microwave-absorbing medium (delivered by atomiser both onto the empty mould cavity and onto the bed of pre-expanded beads), and exposure to 2.45 GHz microwave radiation. The key process parameters were the dose of water, the volume of pre-expanded polystyrene, and the duration of microwave sintering. The results showed that longer sintering times enhanced the flexural strength of the patterns: the highest flexural strength of 127.84 kPa was obtained for a flexural specimen produced with 8 ml of water in 20 cm³ of pre-expanded EPS K-950w/S4311 and a microwave exposure time of 480 s (group mean 125.63 ± 2.99 kPa, n = 3). EPS K-950w/S4311 was more amenable to microwave sintering than Styropor P 426 Ccycled. The current findings establish a robust laboratory-scale framework; subsequent research will focus on scaling these parameters for industrial high-volume production and on broadening the statistical sample base. Overall, the proposed microwave sintering technology shows significant promise for the small-batch and prototype production of casting patterns, offering a more environmentally friendly and cost-effective alternative to conventional autoclave-based steam-chest moulding.

Keywords: Expanded polystyrene, Microwave sintering, Lost Foam casting, Bending strength, Innovative foundry technologies

1. Introduction

The use of foamed macromolecular models for casting dates back to 1958, when H. F. Shroyer patented the use of a polystyrene pattern to replicate casting shapes [10, 12]. Large-scale production of such castings has been conducted since 1987 in the United Kingdom, France, the United States, and Germany. Lost-foam technology is widely applied in the automotive industry, offering an alternative to permanent mould and pressure die casting. This technology is advantageous owing to its low production and capital costs, especially when compared with traditional casting techniques. Critical factors in the lost-foam casting process include the density of the polystyrene pattern, the refractory coating and its thickness, the mould density, and the pressure within the mould.

Expanded polystyrene (EPS), commonly known as polystyrene foam, is a thermoplastic polymer produced as granules saturated with a foaming agent [10]. At the core of each granule resides the foaming agent, which releases gases, such as NH_3, N_2, and CO_2, upon exposure to elevated temperatures. The sintering mechanism is highly dependent on the type of foaming agent used. Foaming agents are classified as physical or chemical. Physical agents

induce a change in state, whereas chemical agents release gases through decomposition, thereby generating foam. Physical foaming agents include gases that dissolve under pressure in the material, as well as solids and liquids that evaporate at elevated temperatures.

Microwave radiation induces intense molecular vibrations and inter-molecular friction, which results in volumetric heat generation [4, 6–7, 14]. This principle is exploited in microwave selective sintering (MSS). To couple microwave energy to non-polar polymers such as polystyrene, an absorber phase — for example, carbon nanotubes, carbon black, graphene nanoparticles, or simply a water film — is introduced on or around the granules. The critical processing parameters in MSS are the microwave power, the exposure time, and the mass of the polymer load. The resulting foamed material demonstrates favourable conductivity, structural stability, low density, fire resistance, and good plastic deformability when a conductive coating is used.

MSS also enables the production of foam patterns when water is used as the energy-transfer medium [10]. In a representative procedure, EPS pellets were pre-expanded for 10 min at 90 °C and subsequently cured for 3 h. The conditioned beads were then coated with a thin water film, placed in a PTFE (Teflon) mould, and subjected to a microwave-driven sintering process governed by defined time and power parameters. The reported results indicated improved adhesion between the EPS granules compared with conventional steam-chest moulding (SCM), an approximately two-fold increase in tensile strength relative to SCM patterns, and a more homogeneous internal structure. The process also exhibited higher energy efficiency than SCM.

In SCM, pre-expanded and conditioned EPS beads are pneumatically charged into aluminium moulds and heated with saturated steam. At approximately 110 °C, the beads re-expand and sinter; the mould is then cooled (typically by water spray) and the pattern is carefully demoulded to avoid distortion. The cycle comprises four stages: filling, sintering, cooling, and ejection. Moulds integrated with vacuum, steam, and water-spray circuits are the most effective [1, 3, 10]. SCM can be extended to certain engineering polymers (e.g. EPBT after chemical modification) to produce low-density patterns with good thermal-compressive stability [5, 7, 13]. The energy demand of the process can be reduced by combining hot air with saturated steam, which shortens the steaming time by approximately 32 % and lowers the forming temperature by approximately 16 °C [10].

In practice, the lost-foam route begins with a disposable EPS pattern coated with a refractory ceramic; this coating forms the working surface of the mould. The coated pattern is embedded in unbonded sand, compacted by vibration, and then poured with molten alloy. The liquid metal thermally degrades the polymer pattern, thereby reproducing the target geometry [10]. The method is widely used in the automotive sector and provides an alternative to permanent-mould and pressure die casting while eliminating parting lines, cores, and draft angles; consequently, high dimensional accuracy can be achieved at comparatively low investment and production costs [8, 10]. Coarse sand is typically used, with clay powder as a filler to lower the overall permeability — a condition preferred in lost-foam practice. Key process variables are mould pressure (often controlled as a vacuum), refractory-coating thickness, alloy type, pouring temperature, pattern density, and the permeability of the system [10]. Pattern density governs the evolution of gaseous decomposition products: higher-density patterns generate more gas, and ferrous alloys (owing to higher pouring temperatures) can produce approximately three-fold more gas than aluminium alloys; if not adequately evacuated, elevated gas pressure at the metal front hinders flow and may arrest filling [9–11]. The refractory coating strongly influences surface quality: it must prevent metal penetration into the sand yet remain sufficiently permeable to allow the escape of gases and liquid decomposition products. Too low a permeability increases internal pressure, risking coating rupture and misruns, whereas excessive permeability promotes roughness and metal fins. Coating thickness should not exceed approximately 0.5 mm in order to maintain acceptable filling rates. Reduced-pressure operation in the flask, in the range 90–95 kPa, promotes rapid filling and enables defect-free castings with intricate geometries [10]. Increasing the pouring temperature tends to raise the filling speed but reduces the pressure in the interfacial gas gap; at the same time, it raises gas temperature and viscosity, improving gas filtration through the protective layer — an approach advantageous for thin-walled, complex parts [10]. For short production runs, EPS patterns can be fabricated on hot-wire plotters or CNC machining centres [10]. Building on this background, the present study investigates an innovative microwave-driven sintering process for two types of expanded polystyrene (EPS) and assesses its viability as an alternative pattern-manufacturing technique for the lost-foam casting industry.

2. Materials and methods

2.1. Materials and Mould Preparation

This study used EPS Styropor® P 426 Ccycled®, a polystyrene material manufactured by BASF (Germany), designed for foam product applications owing to its foaming agent content. The material comprised polystyrene, pentane (up to 5.3%), and isopentane (up to 1.4%). The second material, K-950w/S4311, is an EPS that also contains pentane as the foaming agent. The product is supplied as spherical granules with a bulk density of approximately 0.6 g/cm³. The key parameters included a pentane content in the range of 0.3–4.9% and a granule size of 0.4–0.7 mm. The filament used to 3D-print the moulds was Calibram BT, a high-performance polymeric material intended for engineering and industrial applications [2]. Calibram BT was selected specifically for the present microwave-driven process because it is a low-loss, low-permittivity polymer composite that is essentially transparent to the 2.45 GHz microwave radiation employed (loss tangent tan $\delta \ll 0.01$, relative permittivity approximately 2.5–3 in the GHz range, as typical for unfilled engineering thermoplastics). Consequently, the mould wall does not act as a parasitic absorber, so the microwave energy is preferentially deposited in the water film coating the EPS beads rather than in the mould body. This selective coupling is what makes the moulds dimensionally and thermally stable during the sintering cycle and allows the process to be classified as microwave selective sintering (MSS). In addition, Calibram BT exhibits high mechanical strength and thermal stability up to temperatures well above those reached at the

bead–water interface, and good chemical resistance, which together permit repeated use of the printed moulds. EPS-foaming moulds were manufactured in two variants. A stepped mould (overall dimensions: 100 mm × 10 mm × 580 mm) was designed to produce an 81 mm × 81 mm × 32 mm pattern featuring stepped increments of 4, 8, 16, and 32 mm. A multi-cavity mould (190 mm × 98 mm × 40 mm) was fabricated to produce three standardised flexural test specimens, each with dimensions of 121 mm × 23 mm × 10 mm. Figure 1 shows photographs of the stepped mould and the mould used for the flexural tests.

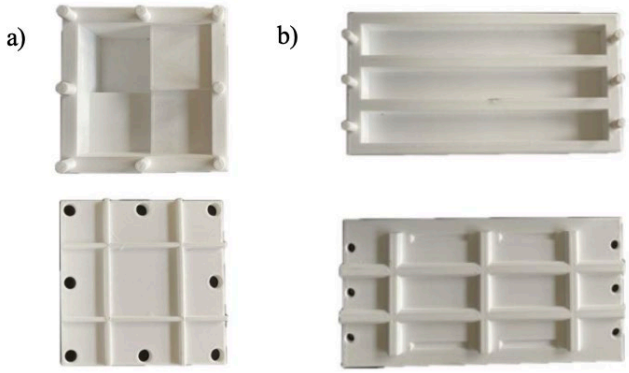

Fig. 1. Molds: a) stepped, b) for bending tests

2.2. Microwave-Driven Sintering Process

Each stage in EPS pattern production by MSS is critical and requires a tightly controlled procedure. The cycle starts with weighing the raw EPS beads and ends with cooling of the mould and demoulding of the finished pattern. The first stage was the pre-expansion of the EPS beads using warm air; this is conceptually analogous to the pre-expansion step of conventional steam-chest moulding (SCM) but uses hot air only, without saturated steam. Water was then applied to the mould in two successive steps, both using a hand atomiser delivering a finely dispersed mist. In the first step the interior of the empty mould cavity was atomised so that a continuous thin water film coated the mould walls. The pre-measured mass of pre-expanded beads was then transferred into the mould, and in the second step the bed of beads inside the mould was atomised with a second metered dose of water (4.8 ml or 9.6 ml for the stepped-pattern experiments, or the bench-scale doses listed in Table 5 for the flexural specimens). Because the two atomiser passes deliver water as a fine spray both at the mould wall and onto the loose bed of beads before the bed is consolidated, the moisture is distributed through the bulk of the charge rather than being limited to the outer surface; this is what allows the microwave field, coupled by the dispersed water film, to act volumetrically through the 32 mm thickness of the stepped pattern. After charging and atomising, the mould was closed and placed in a 1200 W laboratory microwave oven (operating frequency 2.45 GHz). Figure 2 presents a Gantt chart of the complete laboratory-scale process for the fabrication of polystyrene patterns by MSS, broken down into specific stages and the time required for each. The Gantt-chart representation was chosen because it makes the temporal overlap and the dependencies between successive process steps — pre-expansion, conditioning, weighing, mould charging, water atomisation, microwave sintering, cooling, and demoulding — immediately legible, and because it provides a direct visual basis for comparing the total cycle time of the microwave route with that of conventional steam-chest moulding.

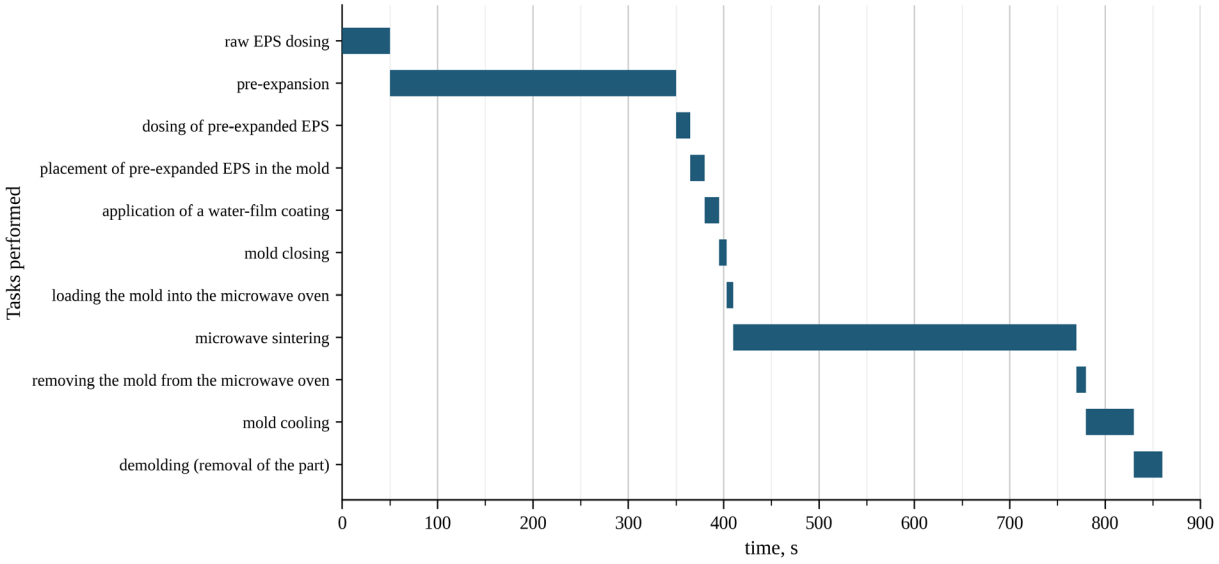

Fig. 2. Gantt chart for laboratory-scale production of EPS polystyrene using MSS technology

Microwave sintering of polystyrene requires input materials such as raw expanded polystyrene (EPS). These undergo several

processing stages to obtain the finished foam patterns. Figure 3 shows a schematic of the laboratory-scale production of foam patterns using microwaves.

2.3. Process Parameter Screening and Optimization

Owing to the innovative nature of utilising microwave radiation for EPS sintering within 3D-printed moulds, standard processing parameters have not been predefined in the literature. Therefore, an extensive preliminary empirical screening was conducted to establish the optimal processing window. The investigation focused on three primary independent variables: the duration of microwave exposure (ranging from 30 to 480 s), the volume of pre-expanded polystyrene, and the amount of water added to the mould.

An iterative optimisation approach was employed, comprising more than 50 preliminary experimental trials. The macroscopic quality of the resulting patterns was evaluated iteratively, with the primary criteria being the degree of particle fusion (sintering quality), structural integrity upon demoulding, and complete filling of the mould cavity. Initial trials identified that insufficient microwave exposure (< 100 s) or inadequate water content failed to initiate the sintering process, whereas excessive parameter values led to incomplete fusion or material degradation. This systematic empirical approach allowed for the precise identification of the boundary conditions and optimal parameter sets, which were subsequently used to produce the final specimens for mechanical and topographical evaluation.

2.4. Surface Topography and Imaging

The topography was measured using a Keyence VR-6000 3D optical profilometer operating in a noncontact mode with a white LED projection. A single scan covered an area of 24 mm × 18 mm, with larger areas obtained by stitching up to 300 mm × 150 mm; the typical acquisition time per scan was approximately 1 s. The system provides a vertical resolution of 0.1 µm and a height repeatability of σ = 0.4 µm. The roughness parameters were evaluated in accordance with ISO 4287 and ISO 25178 standards. Additionally, photographic documentation was acquired using a high-resolution digital imaging system (48-megapixel sensor).

2.5. Mechanical Testing

Mechanical tests were conducted using a Bruker UMT (Universal Mechanical Tester). The mechanical response was evaluated using a three-point bending test configuration on rectangular specimens. The samples were placed on a prism fixture mounted for flexural strength measurements, using a support span length of 80 mm. A force sensor with an accuracy of 0.1 N was utilised, and the tests were performed at a crosshead speed of 2.0 mm/min. The flexural stress σ_f was calculated based on the applied load F_z, following the standard Euler-Bernoulli beam theory equation (1):

$$(\sigma_f) = \frac{3F_z L}{2bd^2} \tag{1}$$

where F_z represents the applied load at the centre of the span (N), L is the support span length (mm), b is the specimen width (mm), and d corresponds to the specimen thickness (mm).

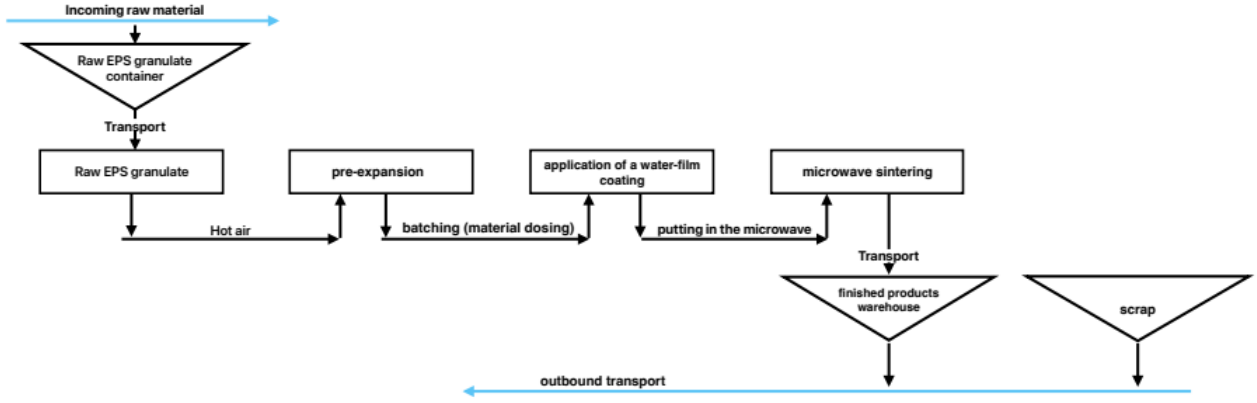

Fig. 3. Schematic of experimental setups to produce foam patterns using microwave radiation on a laboratory scale

3. Results and analysis

3.1. Structural and Topographical Analysis

Surface area analysis of the pre-expanded material (hot air method) was conducted using the ImageJ software. The acquired optical micrograph was imported, scaled, and filtered to identify the particle edges. Figure 4 shows the pre-expanded material with visualised edges, revealing 180 distinct particles.

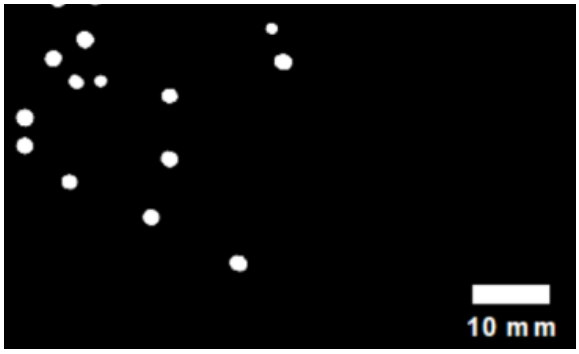

Fig. 4. Pre-expanded EPS

The identified contours were subsequently analysed using the particle area measurement function in ImageJ. Table 1 presents the key statistics for the surface area of the pre-expanded EPS.

Table 1.
Statistics of pre-expanded EPS

Metric	Value
Number of particles (count)	180
Mean (mm²)	2.96
Standard deviation (mm²)	0.69
Minimum (mm²)	1.56
Maximum (mm²)	4.44
Median (mm²)	3.02

Based on the preliminary parameter screening, the most critical factors for microwave sintering of foam patterns were identified as time, water content, and the amount of pre-expanded polystyrene. For the stepped mould, the optimal parameters established during the iterative trials were 4.8 ml of water, 45 cm³ of pre-expanded polystyrene, and a sintering time of 360 s (at a microwave power of 1200 W). Notably, material K-950w/S4311 exhibited superior processing properties, requiring lower input quantities to achieve complete fusion than Styropor P 426 Ccycled.
Figure 5 shows the macrostructures of two EPS K-950w/S4311 samples produced using a stepped mould.

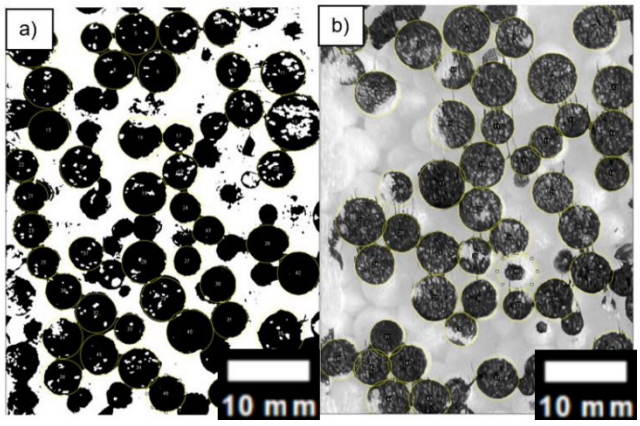

Fig. 5. EPS K-950w/S4311 structure: a) sample 1, b) sample 2

Sample 1 was sintered using 4.8 ml of water, 45 cm³ of pre-expanded polystyrene, for 360 s. Sample 2 was processed using 9.6 ml of water, 45 cm³ of pre-expanded polystyrene, for 480 s. After imaging, both samples were cropped to the same size and region of interest in ImageJ, with 45 particles marked for comparison.
Table 2 presents the surface-area statistics for Sample 1, derived from 45 segmented beads (mean 4.81 ± 1.40 mm² (SD), minimum 2.82 mm², maximum 9.95 mm², median 4.70 mm²).

Table 2.
Statistical data for sample 1

Metric	Value
Number of particles (count)	45
Mean (mm²)	4.81
Standard deviation (mm²)	1.40
Minimum (mm²)	2.82
Maximum (mm²)	9.95
Median (mm²)	4.70

Table 3 presents the surface-area statistics for Sample 2 (45 segmented beads; mean 5.61 ± 1.39 mm² (SD), minimum 2.97 mm², maximum 8.20 mm², median 5.36 mm²). Sample 2 exhibited a larger average bead surface area than Sample 1. It should be emphasised that Sample 1 and Sample 2 are both stepped-mould specimens (45 cm³ of pre-expanded EPS in the stepped cavity) and that they differ from each other in two simultaneously varied parameters: the microwave exposure time was increased from 360 s to 480 s, and the water dose was doubled from 4.8 ml to 9.6 ml. The two variables act synergistically rather than independently — the additional water increases the available dipolar absorber mass at 2.45 GHz, which raises the rate at which microwave energy is converted to heat at the bead surfaces, while the longer exposure time provides more cumulative thermal energy for bead re-expansion and inter-bead fusion. The preliminary parameter-screening trials described in Section 2.3, in which water content and exposure time were varied independently within the ranges 4.8–9.6 ml and 30–480 s, indicate that, within the investigated window, exposure time is the dominant factor for the resulting bead surface area, whereas the water dose primarily controls whether sintering is initiated at all; once a sufficient water film is present, further increases in water dose produce only a moderate additional increase in bead expansion. A formal statistical decomposition of the two effects (e.g. by two-way ANOVA) is beyond the scope of this proof-of-concept paper and will be addressed in a dedicated design-of-experiments study planned as a follow-up.

Table 3.
Statistical data for sample 2

Metric	Value
Number of particles (count)	45
Mean (mm²)	5.61
Standard deviation (mm²)	1.39
Minimum (mm²)	2.97
Maximum (mm²)	8.20
Median (mm²)	5.36

Based on a selected specimen, noncontact 3D scans were acquired with a Keyence VR-6000 profilometer to characterise the

surface roughness and texture, including the profile (Ra, Rz) and areal parameters. Across 61 profiles (five sampling lengths per profile; λ_s= 8 µm, λ_s= 0.8 mm; end-effect correction enabled), the arithmetic mean roughness Ra was 12.13 ± 2.81 µm (range: 8.23–20.71 µm), while the average maximum height Rz was 84.44 ± 18.91 µm (range: 55.74–137.64 µm). A high Rz/Ra ratio indicates pronounced extremes (sharp peaks and deep valleys), implying stress concentrations and uneven real contact areas.

Figure 6 shows the total profile along the measured line, illustrating the height variations around the mean line with pronounced negative excursions.

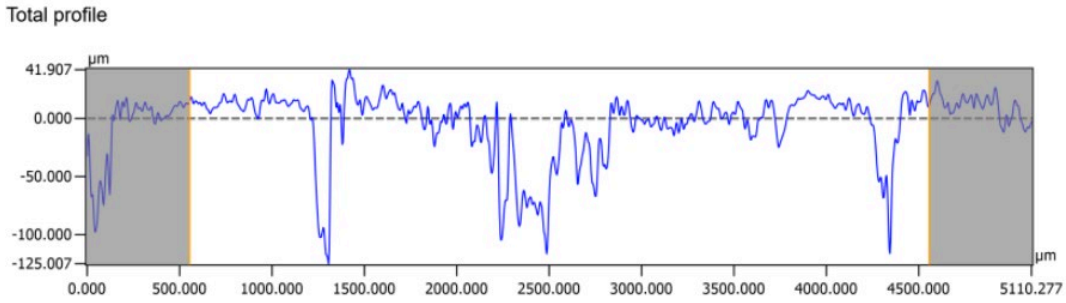

Fig. 6. The total profile along the measured line

This indicates that only the central segment between the orange markers (grey margins excluded) was utilised for the evaluation. Figure 7 provides a 3D view of the polystyrene (PS) surface with height variations, where colours encode the elevation from low (blue) to high (red). Over the evaluated interval, the peak-to-valley height (Max–Min) reached 3.542 mm, indicating a pronounced macrorelief driven by the inherent bead morphology of the EPS surface. The PS cross-section exhibited dual-scale roughness: a macrorelief of dome-shaped beads superimposed on a micro-roughness with pronounced extremes, resulting in local stress concentrations and anisotropic contact.

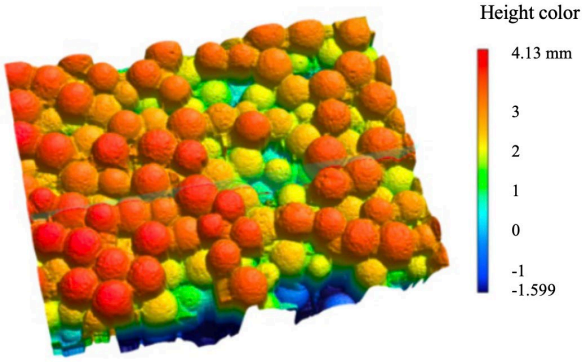

Fig. 7. 3D view of the polystyrene (PS) surface

The height-resolved- segmentation of the convex features yielded a cumulative protrusion volume of 4.86 mm³ over a total measured area of 153.485 mm². The mean per-feature- metrics were 0.02 mm³ in volume, 0.634 mm² in cross-sectional- area, and 0.632 mm² in surface area, with characteristic heights in the tens of micrometres (mean height 0.028 mm; maximum per feature 0.177 mm). These values quantitatively substantiate the densely packed, dome-like bead morphology. Table 4 summarises the volume and area-based metrics of the convex features obtained from the topographical segmentation.

Table 4.
Volume- and area-based metrics of convex features segmented from the PS topography

	Volume (mm³)	Cross-sectional area (mm²)	Surface area (mm²)	Mean height (mm)	Max height (mm)
Total	4.86	154.163	153.485	6.92	13.956
Maximum	0.058	1.909	1.934	0.046	0.177
Minimum	0	0.001	0	0	0
Mean	0.02	0.634	0.632	0.028	0.057

3.2. Mechanical Properties

To determine the flexural strength, the samples were subjected to a three-point bending test by applying an incrementally increasing force until fracture. A total of 22 polystyrene samples with varying input parameters were examined. The experiments confirmed that the amount of water significantly affected the mechanical response; insufficient water failed to initiate adequate sintering, resulting in poor inter-particle fusion and consequently lower strength. Microwave sintering time also exerted a dominant impact, with the longest duration yielding the strongest sample. Conversely, combinations of short sintering times and low water contents resulted in structurally weak samples. It should be noted that minor geometrical variations (±1 mm) occurred across the hand-prepared samples, which inevitably influenced the exact quantitative results.

Figure 8 shows the force–time relationship for samples 2.1, 2.2, and 2.3. Sample 2.2 achieved the highest maximum load F_z of 2.5 N. The ultimate strengths of the three samples produced under identical conditions were highly comparable, indicating satisfactory reproducibility of the process.

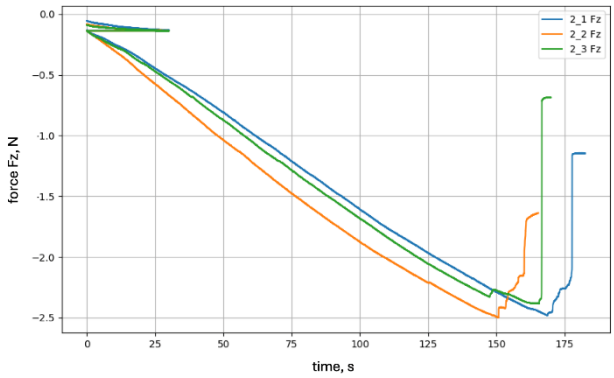

Fig. 8. Relationship between force acting on samples 2.1, 2.2, 2.3 and time

In contrast, Figure 9 illustrates the mechanical responses of samples 5.1, 5.2, and 5.3. Sample 5.3 failed under a negligible force of 0.2 N (the lowest value recorded in this study), attributable to severe over-watering: at 11.2 ml of water in 20 cm³ of EPS the excess free water locally cools the bead surface by latent-heat absorption and prevents proper inter-bead welding, resulting in a structurally weak specimen.

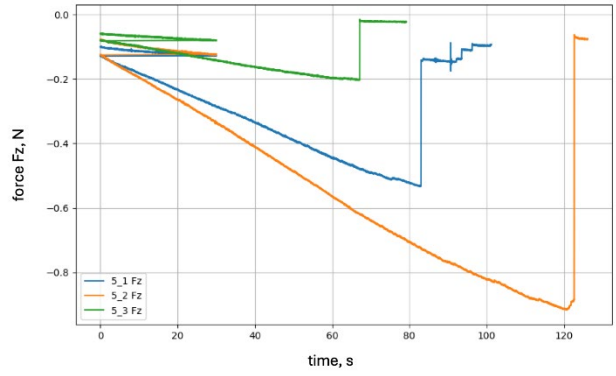

Fig. 9. Relationship between force acting on samples 5.1, 5.2, 5.3 and time

The ultimate flexural strength was calculated from the maximum force at failure. The actual dimensions of the flexural test specimens used in the calculation were: width b = 22 mm, thickness d = 10 mm, and support span length L = 75 mm. Figure 10 presents the combined effect of microwave sintering time and water dose on the flexural strength of EPS K-950w/S4311 specimens produced in the multi-cavity mould (20 cm³ of pre-expanded EPS per specimen). The plotted strength values represent the mean of three nominally identical specimens (n = 3) per experimental group; the individual values, group means and standard deviations are listed in Table 5. One measurement (specimen 7.1) was excluded from the graphical representation because of anomalous macroscopic defects that originated from a localised lack of bead fusion at the mould wall; including this outlier shifted the corresponding group mean by more than one standard deviation, which was judged not to be representative of the investigated processing condition. The compiled data demonstrate two complementary trends. First, for a fixed water dose of 8 ml the flexural strength increases monotonically with microwave exposure time, from 80.97 ± 14.36 kPa at 360 s, through 80.45 ± 11.85 kPa at 390 s and 80.28 ± 27.16 kPa at 450 s, to 125.63 ± 2.99 kPa at 480 s, with the global peak of 127.84 kPa (specimen 2.2) attained at 480 s; the small standard deviation in the 480 s group (CV = 2.4 %) indicates that, under these conditions, the process is also highly reproducible. Second, at a fixed sintering time the strength response to the water dose is strongly non-monotonic: at 360 s the strength is 65.79 ± 37.21 kPa for 3.2 ml water, 80.97 ± 14.36 kPa for 8 ml water and 84.37 ± 20.20 kPa for 6.4 ml water, while at 420 s and 11.2 ml water it collapses to 28.13 ± 18.43 kPa. Mechanistically, an insufficient water dose fails to provide enough dipolar absorber to convert microwave energy into heat at the bead surfaces (under-fusion), whereas an excessive dose floods the bed, locally cools the bead surface by latent-heat absorption, and produces condensate-driven defects. Taken together, Figure 10 identifies a processing window in which a microwave sintering time of 480 s combined with a moderate water dose of approximately 8 ml maximises the flexural strength of the patterns produced in the 20 cm³ multi-cavity mould, and outside which the strength drops sharply. We note that the optimum reported here is geometry-specific: for the stepped pattern (45 cm³ of EPS, 32 mm maximum thickness) the iterative parameter screening of Section 2.3 identified 4.8 ml of water and a microwave sintering time of 360 s as the processing condition giving the most uniform macrostructure, reflecting the lower water dose per unit volume of EPS required for full filling of the larger cavity.

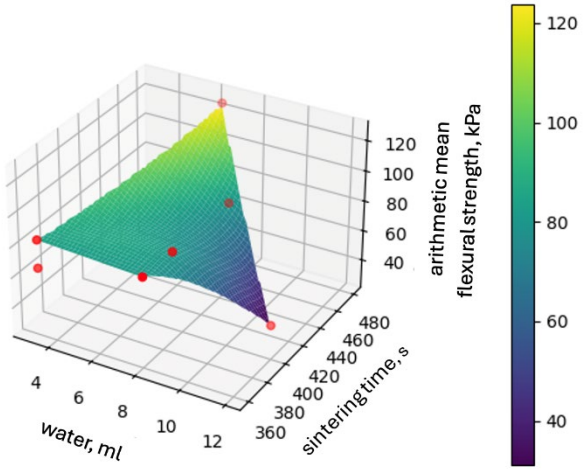

Fig. 10. Graph of bending strength as a function of water content and sintering time

The individual specimens were grouped by processing condition: every experimental group (1–8) corresponds to a single combination of water dose, EPS volume and microwave sintering time, and contains three nominally identical specimens (labelled, for example, 2.1, 2.2 and 2.3 for group 2), tested under identical conditions to assess reproducibility. Table 5 lists each group with its process parameters and the resulting mean flexural strength ± standard deviation; the peak-strength condition (group 2) shows the lowest inter-specimen scatter (CV = 2.4 %), confirming the reproducibility of the optimum.

Table 5.
Flexural strength results by experimental group (mean ± SD, n = 3; group 7: n = 1, outlier)

Group	Water dose (ml)	EPS volume (cm³)	Microwave time (s)	n	Mean strength (kPa)	SD (kPa)	CV (%)
1	8.0	20	390	3	80.45	11.85	14.7
2	8.0	20	480	3	125.63	2.99	2.4
3	6.4	20	360	3	84.37	20.20	23.9
4	3.2	20	360	3	65.79	37.21	56.6
5	11.2	20	420	3	28.13	18.43	65.5
6	8.0	20	360	3	80.97	14.36	17.7
7*	4.8	20	360	1	23.52	—	—
8	8.0	20	450	3	80.28	27.16	33.8

** Group 7 contains only specimen 7.1; the two replicates exhibited macroscopic lack-of-fusion defects and were discarded. Specimen 7.1 is retained here for completeness but excluded from Figure 10 as a defect outlier.*

3.3. Energy Efficiency and Cost Analysis

To substantiate the economic viability of the proposed method, a comparative energy-consumption analysis was carried out between the microwave-driven process and the conventional autoclave route. A standard industrial autoclave requires a high-power input (typically of the order of 40 kW) and operates for approximately 120 s per cycle, which corresponds to an electrical energy consumption of about 1.33 kWh per cycle. The microwave method developed in this study, in contrast, uses a 1.2 kW magnetron operating at 2.45 GHz. For the stepped-pattern process optimum (360 s) the total electrical energy consumed per cycle is about 0.12 kWh, and for the longer 480 s cycle used for the peak-strength flexural specimens it is about 0.16 kWh.

On a per-cycle basis, this corresponds to a reduction in electrical energy demand of about 91 % at 360 s and about 88 % at 480 s relative to the autoclave route. We emphasise, however, that the two routes operate at fundamentally different throughputs. A production autoclave typically processes a full charge of multiple patterns in parallel within a single thermal cycle, whereas the laboratory MSS setup reported here is a single-cavity, single-pattern system. The 88–91 % saving therefore has to be interpreted as energy efficiency per individual prototype or custom pattern, rather than as a direct one-to-one comparison of mass-production cost per part. In this sense the microwave route is positioned not as a replacement of the autoclave for high-volume series production, but as an energy-efficient alternative for the niche of prototype patterns, short pre-series runs, geometrically complex one-off patterns, and small-batch custom castings, where the autoclave is intrinsically over-dimensioned. Even under this restricted framing the operational expenditure reduction is substantial: the dramatic decrease in electrical energy demand translates into a proportional decrease in operating cost per pattern and is accompanied by secondary savings, since the microwave route does not require steam generation, water-spray cooling circuits, or the corresponding utility infrastructure. The data therefore validate the cost-effectiveness and the enhanced energy efficiency of the microwave route specifically for small-batch and prototype lost-foam pattern manufacturing.

4. Conclusion

An innovative method for producing polystyrene patterns using microwave sintering was successfully developed in this study. The research demonstrated that this microwave-driven approach is a viable and efficient alternative to traditional casting pattern manufacturing techniques. The following key conclusions can be drawn based on the conducted experiments:

- The crucial process parameters—sintering time, water content, and material quantity—significantly affect the final mechanical properties of the patterns.
- Longer sintering times promoted the formation of a more cohesive structure, resulting in improved mechanical properties. The highest flexural strength achieved was 127.84 kPa (specimen 2.2), obtained for a microwave sintering time of 480 s combined with 8 ml of water and 20 cm³ of pre-expanded EPS K-950w/S4311 in the multi-cavity flexural mould (group mean 125.63 ± 2.99 kPa, n = 3).
- The optimal water dose is geometry-dependent: 4.8 ml is sufficient for the 45 cm³ stepped pattern at 360 s, whereas the 20 cm³ flexural specimens require approximately 8 ml at 480 s. Excessive water (≥ 11 ml in 20 cm³ specimens) leads to material degradation, condensate-driven defects, and a sharp drop in flexural strength.
- The economic analysis confirmed that the proposed microwave sintering method was more cost-effective than traditional technologies.

Microwave sintering offers new possibilities for prototyping and small-scale production, characterised by high repeatability and efficiency. From an industrial perspective, this method presents the prospect of an alternative manufacturing technology with significant potential for improved energy efficiency and financial savings. However, further comprehensive investigations, particularly for larger-scale components, are warranted to fully exploit this potential in the future.

Acknowledgments

This research received no specific grant from any funding agency in the public, commercial, or not-for-profit sectors. The authors declare that no external funding was received for this study.

References

[1] Brown, J.R. (Ed.). (1988). *Evaporative Foam Casting Technology III* (Paper No. 159). American Foundrymen's Society, Des Plaines, IL.

[2] HMF Chemical. (n.d.). *Calibram BT – material card*. Retrieved June 3, 2024, from https://hmfchemical.eu/en/assets/material-cards/calibram-bt-en.pdf

[3] Cernak, K. (1989). New techniques for making accurate foam patterns. *Modern Casting*. 79(9), 34-35.

[4] Feng, D., Liu, P. & Wang, Q. (2020). Selective microwave sintering to prepare multifunctional poly (ether imide) bead foams based on segregated carbon nanotube conductive network. *Industrial & Engineering Chemistry Research*. 59(13), 5838-5847. https://doi.org/10.1021/acs.iecr.0c00090.

[5] Hossieny, N., Ameli, A. & Park, C.B. (2013). Characterization of expanded polypropylene bead foams with modified steam-chest moulding. *Industrial & Engineering Chemistry Research*. 52(24), 8236-8247. https://doi.org/10.1021/ie400734j.

[6] Jiang, J., Chen, B., Zhou, M., Liu, H., Li, Y., Tian, F., Wang, Z., Wang, L. & Zhai, W. (2023). A convenient and efficient path to bead-foam parts: Restricted cell growth and simultaneous inter-bead welding. *The Journal of Supercritical Fluids*. 194, 105852, 1-12. DOI: 10.1016/j.supflu.2023.105852.

[7] Jiang, J., Wang, L., Tian, F., Li, Y. & Zhai, W. (2023). Polymer bead foams: A review on foam preparation, moulding, and inter-bead bonding mechanism. *Macromol*. 3(4), 782-804. https://doi.org/10.3390/macromol3040045.

[8] Kannan, P., Biernacki, J. & Visco Jr, D. P. (2007). A review of physical and kinetic models of thermal degradation of expanded polystyrene and their application to the lost-foam casting process. *Journal of Analytical and Applied Pyrolysis*. 78(1), 162-171. https://doi.org/10.1016/j.jaap.2006.06.005.

[9] Pacyniak, T. (2007). Effect of foamed pattern density on the lost-foam process. *Archives of Foundry Engineering*. 7(3), 231-236. ISSN (1897-3310).

[10] Pacyniak, T. (2013). *The lost-foam method: selected aspects*. Lodz University of Technology. (in Polish).

[11] Sands, M. & Shivkumar, S. (2003). EPS molecular weight and foam density effects in the lost-foam process. *Journal of Materials Science*. 38, 2233-2239. https://doi.org/10.1023/A:1023700803157.

[12] Shroyer, H.F. (1958). Cavityless casting mold and method of making same. U.S. Patent No. 2,830,343. Washington, DC: U.S. Patent and Trademark Office.

[13] Standau, T., Hädelt, B., Schreier, P. & Altstädt, V. (2018). Development of a bead foam from an engineering polymer with addition of chain extender: Expanded polybutylene terephthalate. *Industrial & Engineering Chemistry Research*. 57(50), 17170-17176. https://doi.org/10.1021/acs.iecr.8b04799.

[14] Standau, T., Zhao, C., Murillo Castellón, S., Bonten, C. & Altstädt, V. (2019). Chemical modification and foam processing of polylactide (PLA). *Polymers*. 11(2), 306, 1-39. https://doi.org/10.3390/polym11020306.